Structural characteristics of the subtropical jet stream and certain lower-stratospheric wind systems

By CHESTER W. NEWTON[1] and ANDERS V. PERSSON[2], *The University of Chicago*[3], *Ill.*

(Manuscript received December 21, 1961)

ABSTRACT

Analyses of the wind field are presented for several cases, which illustrate the considerable variability in structure of the subtropical jet stream. Two cores of strongest wind are common, one lying in the break between the middle and subtropical tropopause and the other often lying above the subtropical tropopause. The layer of strongest wind on the cyclonic flank slopes upward toward north and is often identifiable as a discrete wind-speed maximum several kilometers above the polar-front jet stream. On the anticyclonic flank, the lower subtropical jet slopes downward toward south and is sometimes stronger than the higher-level layer of maximum wind.

Although the broad-scale structure of the wind fields is qualitatively in accord with the solenoid field, large deviations from the thermal wind relationship are found in layers of restricted depth. Measured vertical shears are often double or triple the size of the thermal shear, and in certain regions the thermal and actual shears are of opposite sign. These deviations are shown to be associated with inertial effects arising from curvature of the flow, and from variations of curvature with height.

An example is given illustrating the shallow filaments of strong wind sometimes found in the lower stratosphere above the tropospheric jet streams. These are not indicated by the thermal field, and are evidence of strong domination by inertial effects.

1. Introduction

Despite the considerable amount of attention which has been devoted to the subtropical jet stream and to its role in the general circulation, little has been published relating to its detailed three-dimensional structure. This is undoubtedly due in large part to the sparsity of observations in low latitudes, and to uncertainties in distinguishing real features from the errors inherent in observation of winds at high altitudes and fast speeds. These difficulties have not disappeared, but they have decreased with the vast improvement of observing systems in the last few years.

The purpose of this study is to describe some of the features characteristic of the subtropical jet stream, and to look into the dynamical relationships between the wind and temperature fields. In particular, the role of inertial influences will be examined.

As emphasized by Saucier and collaborators (1958), no single "model" is representative of the structure of the jet stream or of the accompanying thermal fields. The present discussion is not intended in that light, although an attempt will be made to summarize the principal features which are commonly observed.

2. Structure on January 15, 1959

The subtropical jet stream on January 15, 1959 will be examined in some detail at the outset, because its structure was particularly simple at that time. This case will serve to bring out some salient physical features, variations in structure being illustrated later on.

At 1500 GCT January 15, 1959 (Fig. 1), the subtropical jet stream was well removed from the polar-front jet over eastern North America. This fact permits a clear view of the separate currents, shown in cross section in Figs. 2 and 3.

---

[1] Now at National Severe Storms Project, U. S. Weather Bureau, Kansas City, Missouri.

[2] Now at Swedish Meteorological and Hydrological Institute, Stockholm, Sweden.

[3] Research supported by The Office of Naval Research (Contract Nonr 2121(10), 082-161, and The National Science Foundation (Grant NSF-G6353).

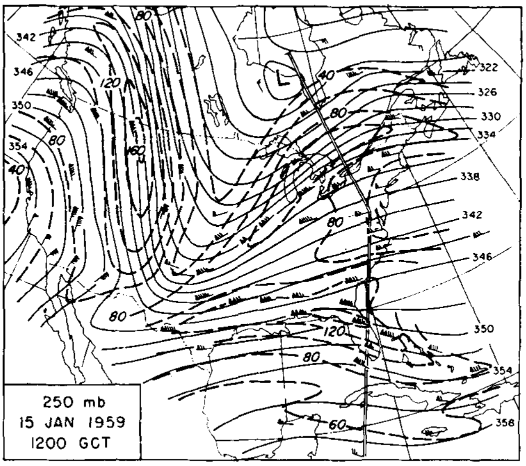

FIG. 1. Contours (solid lines, heights in hundreds of ft) and isotachs (broken lines, speeds in knots) at 250 mb, 12 GCT January 15, 1959.

In the construction of this and the following sections, wind and temperature data were utilized both from teletype reports and from checked data in the Northern Hemisphere Data Tabulations published by the United States Weather Bureau. By combining data from both sources, fairly complete velocity profiles could be constructed. The wind observations shown in Fig. 3 are representative of the amount of information available. In general, this is bolstered by other observations upstream or downstream from the cross sections. Multiple-level wind maxima appearing on the sections were in general given credence only when supported by several stations.

General features of wind and temperature fields. The principal features of interest in this example are as follows:

(1) Viewing the subtropical jet stream in

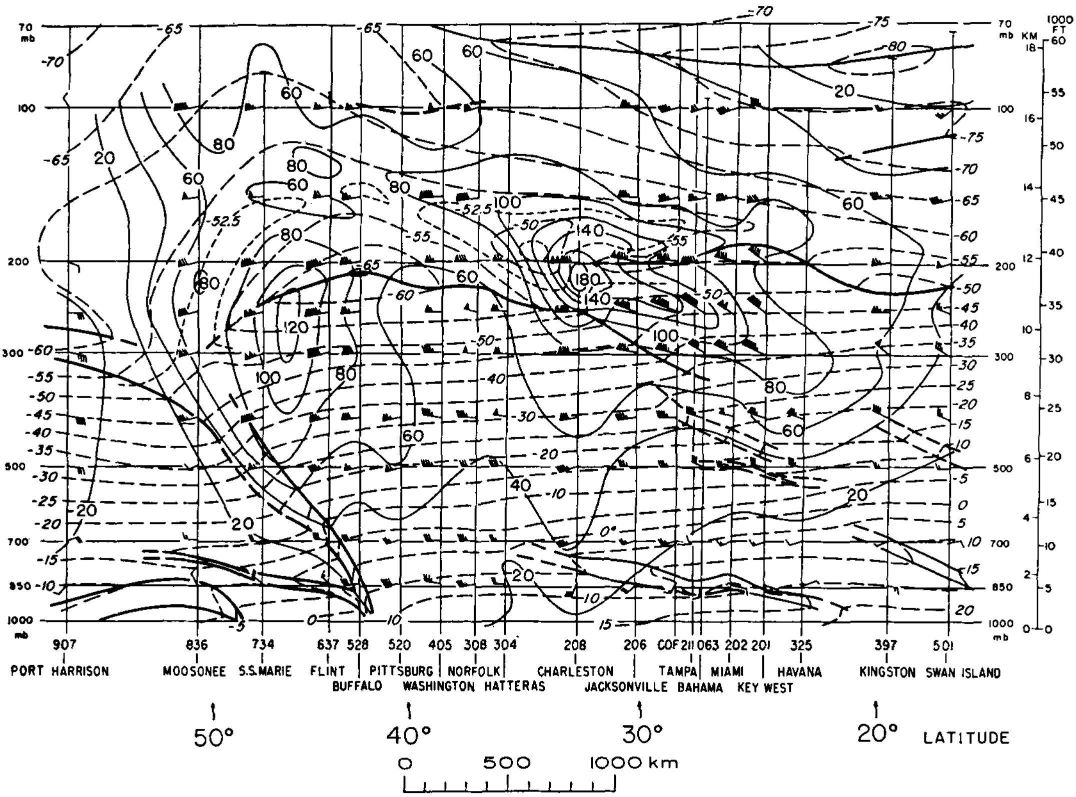

FIG. 2. Vertical section along double line on Fig. 1. Isotherms, dashed lines (°C, slanted numbers); isotachs, thin solid lines (knots, upright numbers); heavy lines mark stability discontinuities at frontal boundaries and tropopauses. Winds plotted with reference to north at top of page. In this and following sections, isotachs are for total wind speed.

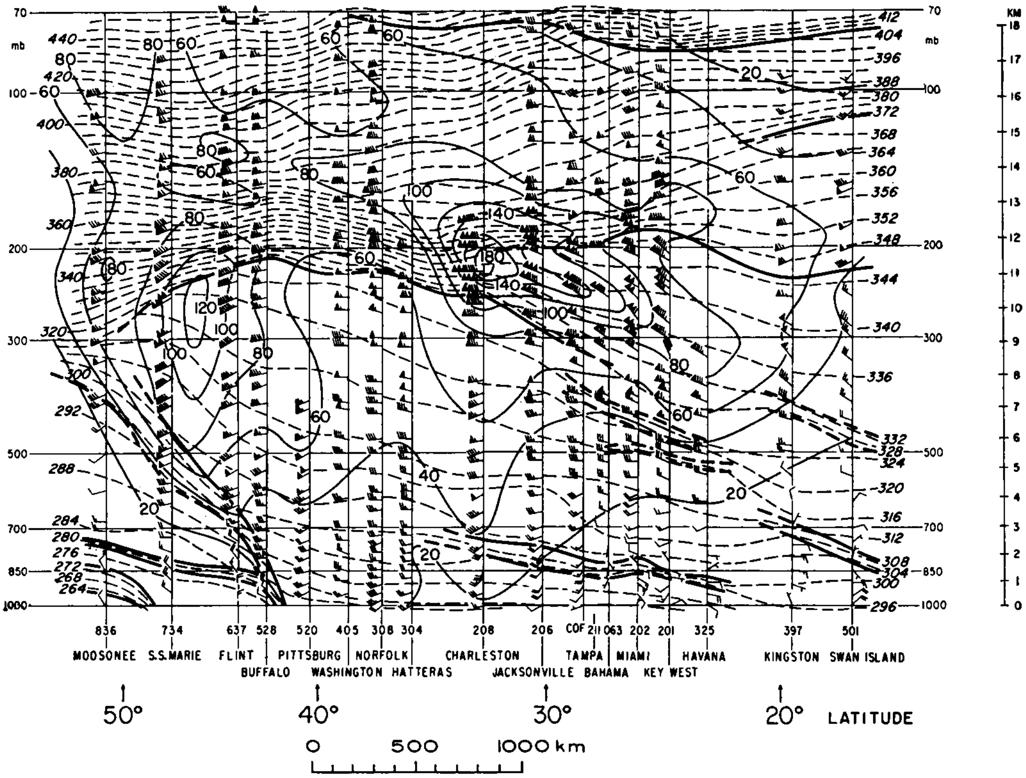

FIG. 3. Same section as in Fig. 1. Dashed lines are isentropes (°K).

broad scale, the layer of maximum wind (LMW) was tilted downward toward south.

(2) This LMW extended in a continuous sheet for at least 1400 km north of the jet axis, lying well above the tropopause over the polar-front jet stream.

(3) On the south side, two levels of maximum wind were present, the lower one sloping downward toward south being strongest in this case. The lower LMW (Fig. 3) appears to lie nearly on an isentropic surface, south of the jet axis.

(4) Like the polar-front jet, the subtropical jet lies in the region of a break in the tropopause.

(5) North of this tropopause break, a layer of warm air sloped upward into the stratosphere, overrunning the band of cold air associated with the highest part of the tropopause south of the polar-front jet. The LMW north of the subtropical jet lay just above the layer of highest stratospheric temperature.

(6) The tropopause between the polar-front jet and the subtropical jet appeared to be a single continuous sheet, extending south of the subtropical jet axis as the base of a layer of gradually weakening stability.

In accordance with the terminology of Defant and Taba (1957), the latter tropopause will be called the "middle" tropopause. The stable layer beneath the subtropical jet will be called the "subtropical front", after Mohri (1953), and the tropopause south of the subtropical jet (near 200 mb) the "subtropical tropopause".

Our analyses support Mohri's view that the base of the subtropical front is generally identifiable with the southward extension of the middle tropopause. This interpretation is consistent with the presence of a single lapse-rate discontinuity which could be readily matched at neighboring stations over the portion of North America within the range of latitudes covered by the middle tropopause and the subtropical front. Potential temperatures at the base of the subtropical front were identifiable with those at the middle tropopause, allowing

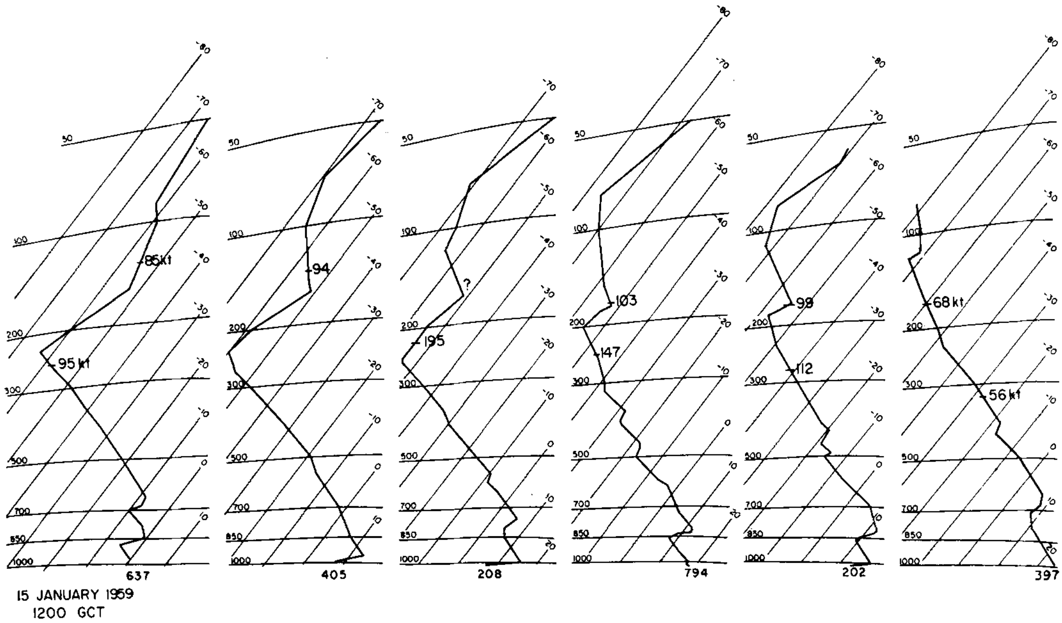

FIG. 4. Temperature soundings plotted on tephigrams, for several stations in Figs. 2 and 3. Numbers are speeds (kt) at levels of maximum wind. At Canaveral (794), the break in lapse rate at 320 mb is the base of the subtropical front, identified with the middle tropopause at stations further north. The break at 200 mb at the same station is the subtropical tropopause, which is only weakly evident at 232 mb at the southernmost station, Kingston (397).

for variations of potential temperature with pressure characteristic of the tropopause itself.[1]

It is also clear that the subtropical and middle tropopauses are distinct entities, since both appear on individual soundings in the transition region at widely differing potential temperatures. This interpretation differs from that of Defant and Taba (1957), based on synoptic-statistical analyses of the mean structure around the hemisphere which were intended to reveal the broad features rather than the detailed structures.

Mohri (1953; 1958) has presented some remarkable examples of the subtropical front over southeast Asia. Occasionally, this front over North America achieves a development comparable with that of the higher-tropospheric polar front, as in Mohri's examples. When it is relatively weak, as in Figs. 2 and 3, the subtropical front generally has a base defined by a distinct lapse-rate break, but a diffuse upper boundary. When strong, the top of the stable layer may also be clearly defined, and the front may be identified as far down as the 500 mb level.

3. Relations between wind and temperature fields

In a broad sense, the presence of strong winds near 200 mb in Figs. 2 and 3 is supported by the thermal field, which shows a northward decrease of temperature in the troposphere and the opposite in the stratosphere. There are, however, significant quantitative and qualitative deviations from the normal relationship between wind and temperature distributions. As observed by Palmén (1948) and Riehl (1948), the middle tropopause is typically highest and coldest some 500 km equatorward from the polar-front jet, as in Fig. 2. The presence of a layer of warm air, sloping upward over this cold band from the latitude of the subtropical jet stream, provides a solenoid field qualitatively consistent with the observed increase of wind with height in a layer 2–3 km above the tropopause. Above the layer

[1] Extraneous stable layers such as those in the middle troposphere between Canaveral (COF) and Havana in Figs. 2 and 3 are common, and are not identified with the subtropical front. They may, however, contribute an appreciable part of the total baroclinity within the troposphere.

of warmest air, the horizontal temperature gradient reverses. As seen from Fig. 2 and the sample of soundings in Fig. 4, the observed winds reached greatest strength a little above the level of highest stratospheric temperature, in close but not exact agreement with geostrophic considerations.

It is evident that there can be no direct connection between the level of maximum wind associated with the polar-front jet and the northward extension of the subtropical jet. This follows from the presence of the cold band over the upward bulge of the middle tropopause (see Fig. 2), north of which the geostrophic wind must decrease and south of which it must increase with height in the lower stratosphere. The presence of two distinct layers of maximum wind between the two jet-stream systems has been noted by Bundgaard and collaborators (1956). They point out that the upper "tropical" wind maximum gradually weakens northward, and that the lower "polar" maximum gradually becomes less distinct southward. Thus where winds are strongest, a level of maximum wind is easily defined, but this is not so in the transition region.

Beneath the jet core and south of it, the vertical shear in a layer 1 to 2 km deep was very strong, despite a relatively weak horizontal temperature gradient. Although the jet was at a low latitude, a check of the observed shear against the geostrophic thermal wind reveals that the former was very much in excess. Such a discrepancy has been noted by several authors.

The presence of a level of maximum wind nearly coincident with a *sloping* isentropic surface south of the jet (Fig. 3) presents a curious aspect, since above the jet the actual and thermal wind shear are opposite in sign. Saucier and collaborators (1958) and Reiter (1960) have found that the level of maximum observed wind sometimes does not coincide with the level of maximum geostrophic wind speed, as deduced from analyses of aircraft reconnaissance flights.

Vertical shear in relation to horizontal temperature gradient and to inertial effects: An expression (BELLAMY, 1941) more general than the geostrophic thermal wind equation may be derived from the equation of horizontal motion,

$$V^2 K_T = f(V_g - V), \tag{1}$$

where V is the actual wind speed, V_g is the component of geostrophic wind parallel to the actual wind, and $K_T = 1/R_T$ is the trajectory curvature (taken as positive for cyclonic and negative for anticyclonic curvature). Taking the derivative with height on both sides of (1) gives directly

$$\frac{\partial V}{\partial z} = \frac{1}{(f + 2K_T V)}\left[f\frac{\partial V_g}{\partial z} - V^2\frac{\partial K_T}{\partial z}\right]. \qquad (2$$

A more general relationship, pertaining to the vector change of wind with height, has been derived by Forsythe (1945).

The actual vertical shear differs from the geostrophic (thermal) shear by virtue of the variation of the centripetal acceleration with height. This may be due either to a variation of speed or of trajectory curvature with elevation. The variation of centripetal acceleration with height is an expression of the circulation acceleration in a plane normal to the wind. This is assumed zero in the thermal wind equation wherein the solenoidal acceleration in such a plane is in equipoise with the Coriolis accelerations.

When $V = 2V_g$, the first factor in (2) can be shown by use of equation (1) to be infinite, and in that case the vertical shear becomes indeterminately large if there is any horizontal temperature gradient at all. Bjerknes (1951) and others have shown that $V = 2V_g$ is the limiting value that the wind speed can reach while satisfying gradient motion (parallel to the isobaric contours). We have been unable to find any cases where this limit is closely approached in the subtropical jet stream. Nevertheless, any significant approach to it strongly affects the vertical shear. For example, when the actual wind is only $\frac{1}{3}$ larger than the geostrophic wind, the vertical shear is double the thermal shear. This condition is not uncommon.

By substitution from the thermal wind equation $\partial V_g/\partial z = g(fT)^{-1}(\partial T/\partial n)_p$ into equation (2), the criterion for the real vertical shear to be opposite in sign to the thermal wind is found to be

$$V^2\frac{\partial K_T}{\partial z} > \frac{g}{T}\left(\frac{\partial T}{\partial n}\right)_p. \tag{3}$$

Here n is taken positive to right of the wind. Even if the air is warmest to right, the real wind can decrease upward if large enough wind

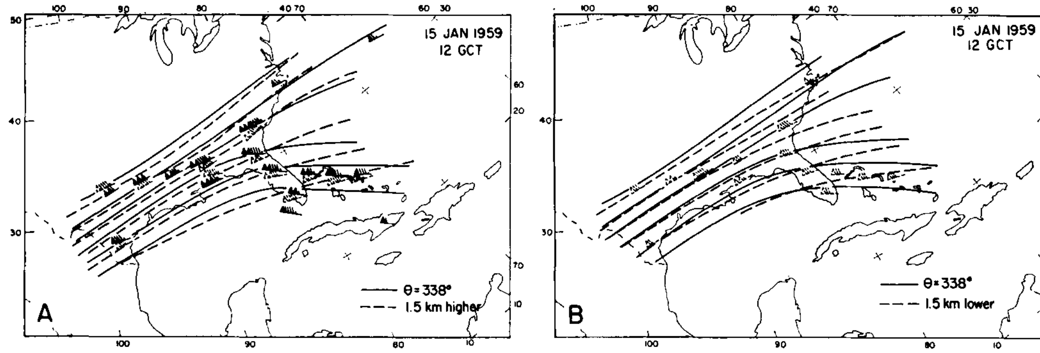

FIG. 5. (*a*) Observed winds and streamlines at 338°K isentropic surface (solid wind symbols and lines), and 1500 m above that surface (dashed). (*b*) Streamlines at 338°K surface (solid), and winds and streamlines (dashed) 1500 m below that surface.

speeds are combined with a sufficient increase of cyclonic curvature (or decrease of anticyclonic curvature) with elevation. With any significant temperature gradient (say 5°C per 1000 km), the required speeds and curvature variations are appreciable. Such conditions are only met in layers of limited depth, so that the *broad-scale* distribution of winds is qualitatively controlled by the thermal field.

At Charleston in Fig. 2, the reported wind increased by about 100 kt in less than 1 km above the tropopause, It has proved beyond the power of the authors to account for this extreme shear within the framework of the equations of motion, without casting aspersions upon the accuracy of the measured winds. Prudence therefore dictates that we divert the attention of the reader to the other stations just south.

The mean observed shear between 250 and 300 mb (below the level of maximum wind) at Jacksonville, Canaveral (COF) and Bahama was 23 m/sec per km. In the same layer the thermal shear was only 9 m/sec per km. Thus the observed shear was over $2\frac{1}{2}$ times as large as the thermal shear.

In order to evaluate the curvatures in equation (2), the winds were examined at the 338°K isentropic surface where winds were strongest, and 1.5 km above and below that surface. As seen in Fig. 5, the anticyclonic curvature was strongest at the level of maximum wind, with appreciable variation of curvature with height particularly above that level.[1]

[1] Actually, expression (3) shows that if the thermal wind is positive at the level of maximum wind, strongest anticyclonic curvature must be present somewhat below that level.

Sparing the reader the details of the computations (an example of which will be given later on), we simply state that in the region mentioned above the shear computed from (2) was 21 m/sec per km, in close agreement with the observed shear. Above the level of maximum wind, the thermal shear was +9.5 m/sec per km while the observed shear was −8 m/sec per km. The computed value from (2) was −3 m/sec per km. The evaluation of equation (2) is quite sensitive to the precise values adopted for its individual constituents, particularly when the bracketed terms are opposite in sign and appreciable in size. This degree of agreement must be considered acceptable in the light of the limited observational data available in this locality.

By interpretation of equation (1), the ratios

$$\frac{(V - V_g)}{V_g}; \quad \frac{(\partial/\partial z)(V - V_g)}{\partial V_g/\partial z}$$

provide a measure of the influence of inertial motions (i.e., centripetal accelerations) relative to the geostrophic control of wind speeds. From the above computations, the latter ratio averages 165 per cent above and below the level of maximum wind, compared with an average value of 36 per cent for the former, in the same layers. Thus while inertial effects have a considerable but not dominant influence on the wind speeds at a given level, they overwhelmingly dominate the vertical shear. This is true, of course, only at levels where the wind as well as the shear is strong, since the centripetal acceleration and its variation with height depend strongly on the magnitude of the wind speed.

Shape of the vertical profile of wind speed: Palmén (1948) has shown that if there is a discontinuity of horizontal temperature gradient across a sloping surface, there is also a discontinuity in the geostrophic horizontal wind shear. This statement is valid not only at the surfaces bounding frontal layers, but also at sloping tropopauses such as the one at the base of the subtropical front. The strength of such a shear discontinuity is proportional to the difference in the temperature gradients and to the slope of the discontinuity surface, both of which are small in the case of Fig. 2, but in some cases the discontinuity of horizontal shear across the subtropical front boundary is quite strong.

Palmén's statement is naturally also true of the vertical shear. Subtracting the thermal wind equation corresponding to one side of a stability discontinuity (primed quantities) from that corresponding to the other side (unprimed),

$$\frac{\partial u_g}{\partial z}-\frac{\partial u_g'}{\partial z}=-\frac{g}{f\theta}\left(\frac{\partial \theta}{\partial y}-\frac{\partial \theta'}{\partial y}\right),$$

where y is positive to the left of the intersection of the discontinuity surface with an isobaric surface. If $\psi=\delta z/\delta y$ is the slope of an isentropic surface,

$$\psi\frac{\partial \theta}{\partial z}=-\frac{\partial \theta}{\partial y}.$$

Analyses show that the tropopause at the base of the subtropical front, although not strictly an isentropic surface, can be considered as such for the purposes of a qualitative discussion. With this approximation, substitution of the latter expression into the former gives

$$\frac{\partial u_g}{\partial z}-\frac{\partial u_g'}{\partial z}\approx\frac{g}{f\theta}\left(\frac{\partial \theta}{\partial z}-\frac{\partial \theta'}{\partial z}\right)\psi, \tag{4}$$

where ψ is now interpreted as the slope of the discontinuity surface. For practical purposes, u_g may be considered as the total geostrophic wind speed.

The stability discontinuity across the sloping tropopause beneath the subtropical jet must then also be a discontinuity in the vertical (thermal) shear. Leaving aside variations of curvature with height, substitution from (2) would give

$$\frac{\partial V}{\partial z}-\frac{\partial V'}{\partial z}\approx\frac{g}{(f+2K_TV)\theta}\left(\frac{\partial \theta}{\partial z}-\frac{\partial \theta'}{\partial z}\right)\psi. \tag{5}$$

Thus the discontinuity of shear would be accentuated in the case of anticyclonic flow.

An approach to a shear discontinuity is suggested by the profiles of wind speed (Fig. 6) at Charleston (208) and Montgomery (226), at both of which stations there was a distinct lapse-rate discontinuity. However, it is in principle not possible to detect a distinct discontinuity of shear because of the necessary practice of computing average winds over a finite time of a balloon's ascent. Such an averaging not only vitiates discontinuities, but makes the wind appear to increase somewhat below the level where an actual increase takes place.

Where there is no discontinuity in lapse rate, the shape of the geostrophic wind profile can be inferred from the expression

$$\frac{\partial^2 V_g}{\partial z^2}=\frac{g}{f}\left(\frac{\partial S}{\partial n}\right)_p, \tag{6}$$

obtained directly by taking the vertical derivative of the thermal wind equation. Here $S=\theta^{-1}\partial\theta/\partial z$ is the vertical stability. According to (6), at levels where there is greater stability to the right of the wind, the geostrophic vertical shear increases in magnitude with height.

As shown by Fig. 6, a concave shape characterizes the wind profiles beneath the jet, where such a stability distribution is observed. When anticyclonic flow is present, the curvature of the vertical speed profile may be considerably stronger than indicated by (6), being multiplied up by a factor $f/(f+2K_TV)$ if variations of horizontal curvature with height are neglected.

At the level of maximum geostrophic wind, (6) shows that weaker stability must lie to right of the jet core, or that the isentropes in a vertical section must diverge toward right. This condition is met, as in the case of the polar-front jet stream, when the left flank of the subtropical jet lies in the stratosphere and the right flank in the troposphere, with a break in the tropopause across the jet axis. The presence of significant variations of curvature with elevation com-

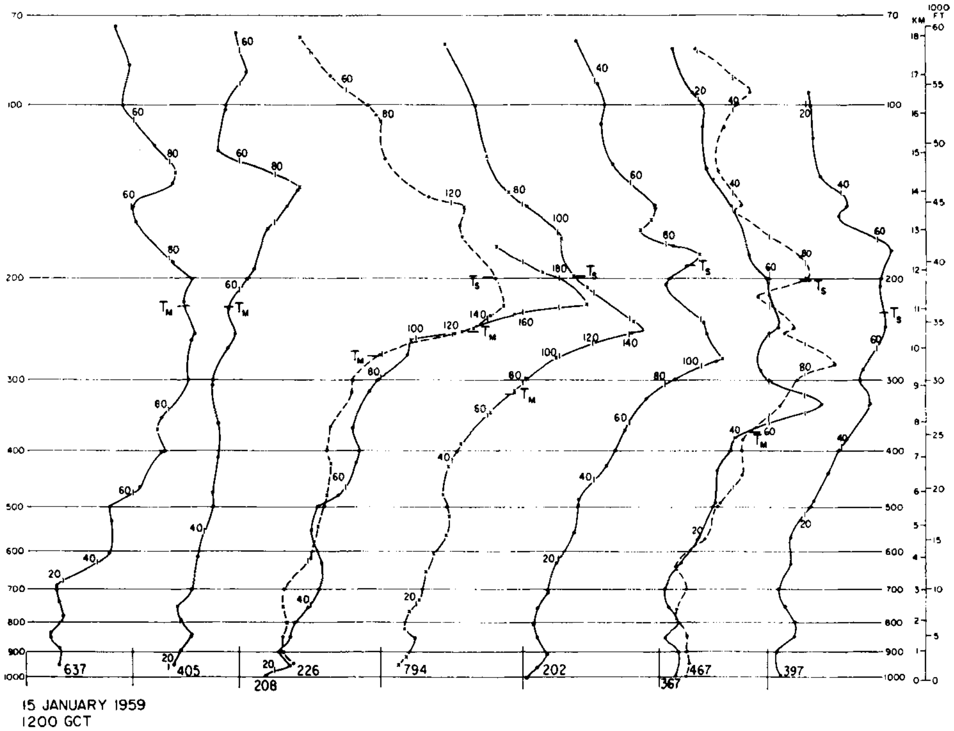

FIG. 6. Profiles of wind speed at selected stations on or near cross section in Figs. 2 and 3. Numbers beside individual curves indicate speed (kt). T_m and T_s indicate levels of middle and subtropical tropopauses. Guatanamo (367) and Sabana del Mar (467), east of section, show two layers of strong wind probably also present at Havana.

plicates the situation in reality, and the above discussion is strictly applicable only to the geostrophic wind field.

4. Some variations in structure

As noted earlier, the structure of the subtropical jet varies a great deal, although certain physical features tend to be conserved. Two examples showing such variations are shown in Figs. 7 and 8.

Referring back to Fig. 2, it was noted that on January 15, 1959 there were two layers of maximum wind south of the main jet core, one above and one below the subtropical tropopause near 200 mb. Comparing Fig. 7, on March 29 1960 two distinct jet cores are noted near 30° latitude.[1]

The one above the subtropical tropopause was in this case stronger at all latitudes, and again a layer of maximum wind extended from the subtropical jet past the northern end of the section at 2–4 km above the middle tropopause. South of the jet core, there were again sheets of stronger winds, which appear to be identified with sloping isentropic surfaces. These bear no evident relationship to the thermal field, which also furnishes no clue to the structure of the wind field near the jet cores. It is further noted that the northward extension of the layer of maximum wind was somewhat above the layer of warm air that sloped upward into the stratosphere north of the subtropical jet. All these features bear evidence that inertial effects strongly influence the detailed structure of the wind field.

Fig. 8 illustrates the kind of complicated structure observed when the subtropical and polar-front jets lie close together. Close scrutiny of this figure will reveal that all the principal features (such as the principal tropopauses; warm and cold bands in the lower stratosphere)

[1] Examples of superposed wind maxima similar to this are shown by Saucier and collaborators (1958).

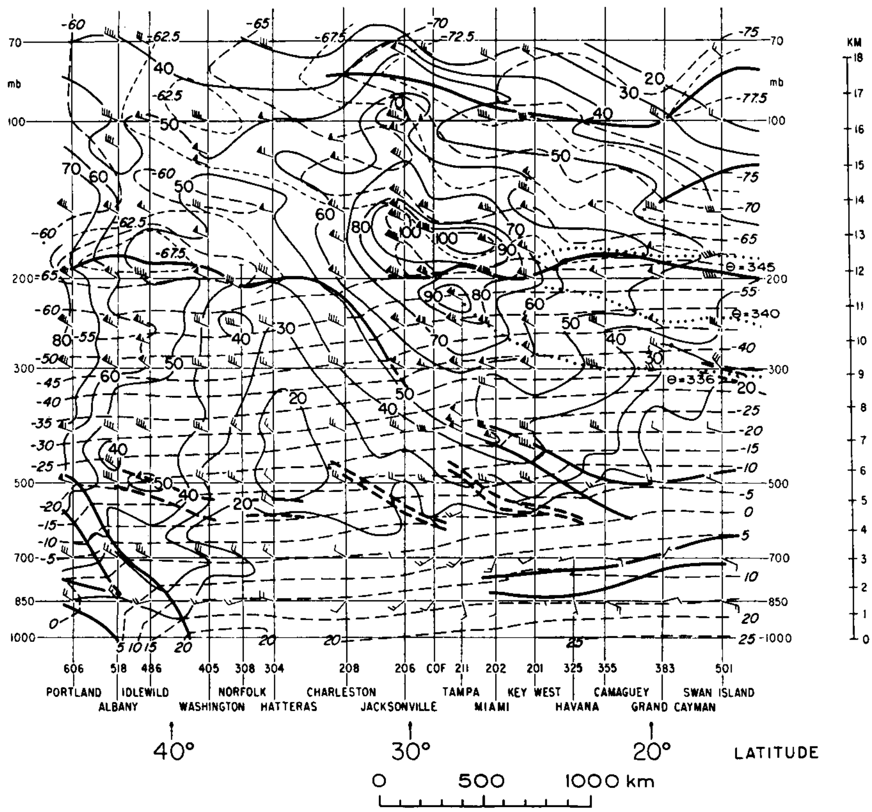

FIG. 7. Temperature and wind distributions near 80° W at 00 GCT March 29, 1960.

were present as in the other sections; they are so strongly compressed laterally that the structure appears very confused. Discrete wind maxima again appear above and below the subtropical tropopause near latitude 30°. The upper of these subtropical jets was probably connected with the layer of maximum wind above the polar-front jet at 120–150 mb, which is poorly related to the thermal field in some places.

An example during the warmer season: Fig. 9 shows the 200-mb chart on September 12, 1960, when the subtropical jet was fairly far north in comparison with its winter location.

The five sections in Fig. 10, along the lines indicated on Fig. 9, show that there were significant variations in structure along the current. In the upstream section (Fig. 10*a*), strongest winds were observed near 200 mb at all stations. Further downstream (Figs. 10*b–d*), the level of maximum wind gradually assumed a strong tilt downward toward south. Finally, east of the trough (Fig. 10*e*) the structure was much the same as in Fig. 10*a*.

Where the level of maximum wind was tilted downward toward south, the subtropical front was quite pronounced, as shown by the soundings in Fig. 11 (corresponding to Fig. 10*d*). A cross section in the trough 24 hr later (not shown) revealed a very strong subtropical front, with higher temperatures at its warm-air boundary than further south. The structures in Figs. 10*c* and 10*d* indicate, as in the cases discussed earlier, a pronounced inertial influence on the wind shear, in spite of the relatively weak winds.

Level of maximum wind in relation to isentropic surface: Väisänen (1954) has examined a number of cases and found indications that the core of the polar-front jet stream tends to follow an isentropic surface. To examine this question in the present case, the wind profiles near the axis of the jet (referring to the jet axis at the

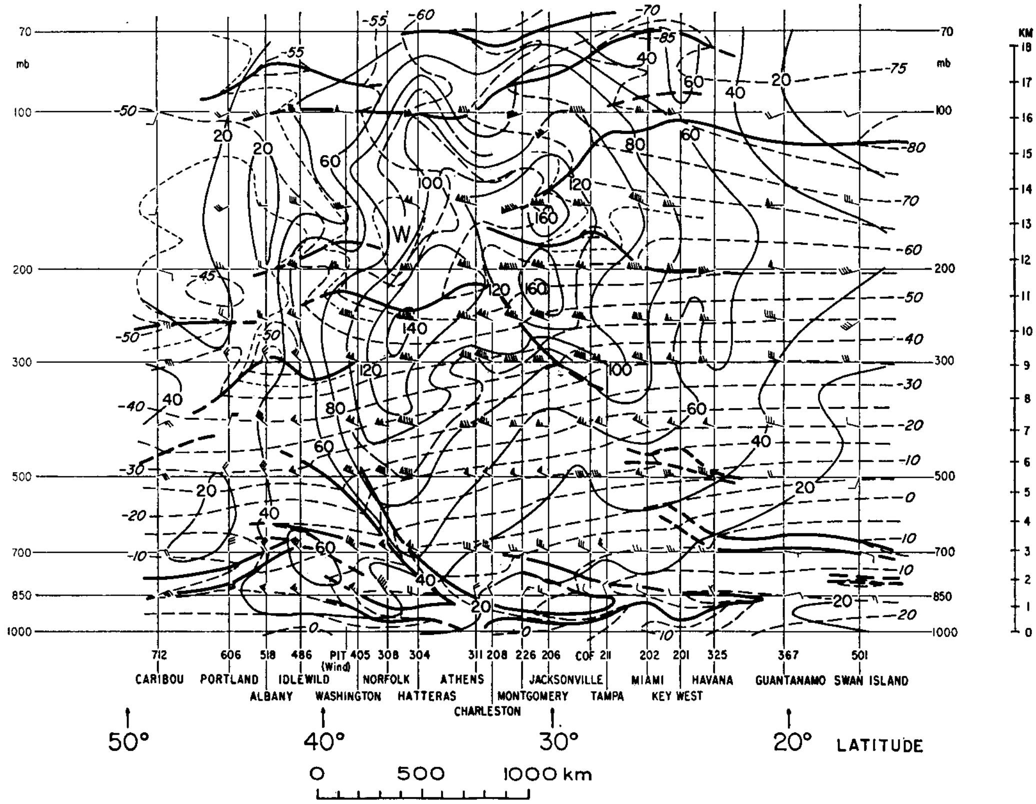

FIG. 8. Temperature and wind distributions near 80° W at 12 GCT February 20, 1960.

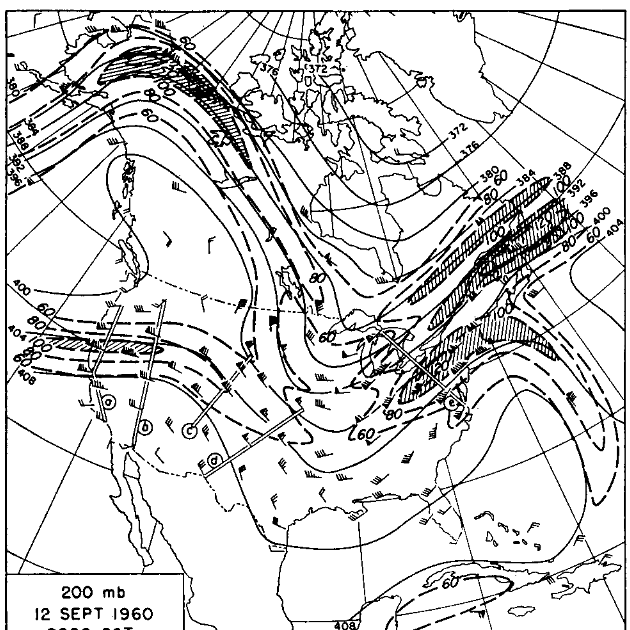

FIG. 9. Contours and isotachs at 200 mb, 00 GCT September 12, 1960.

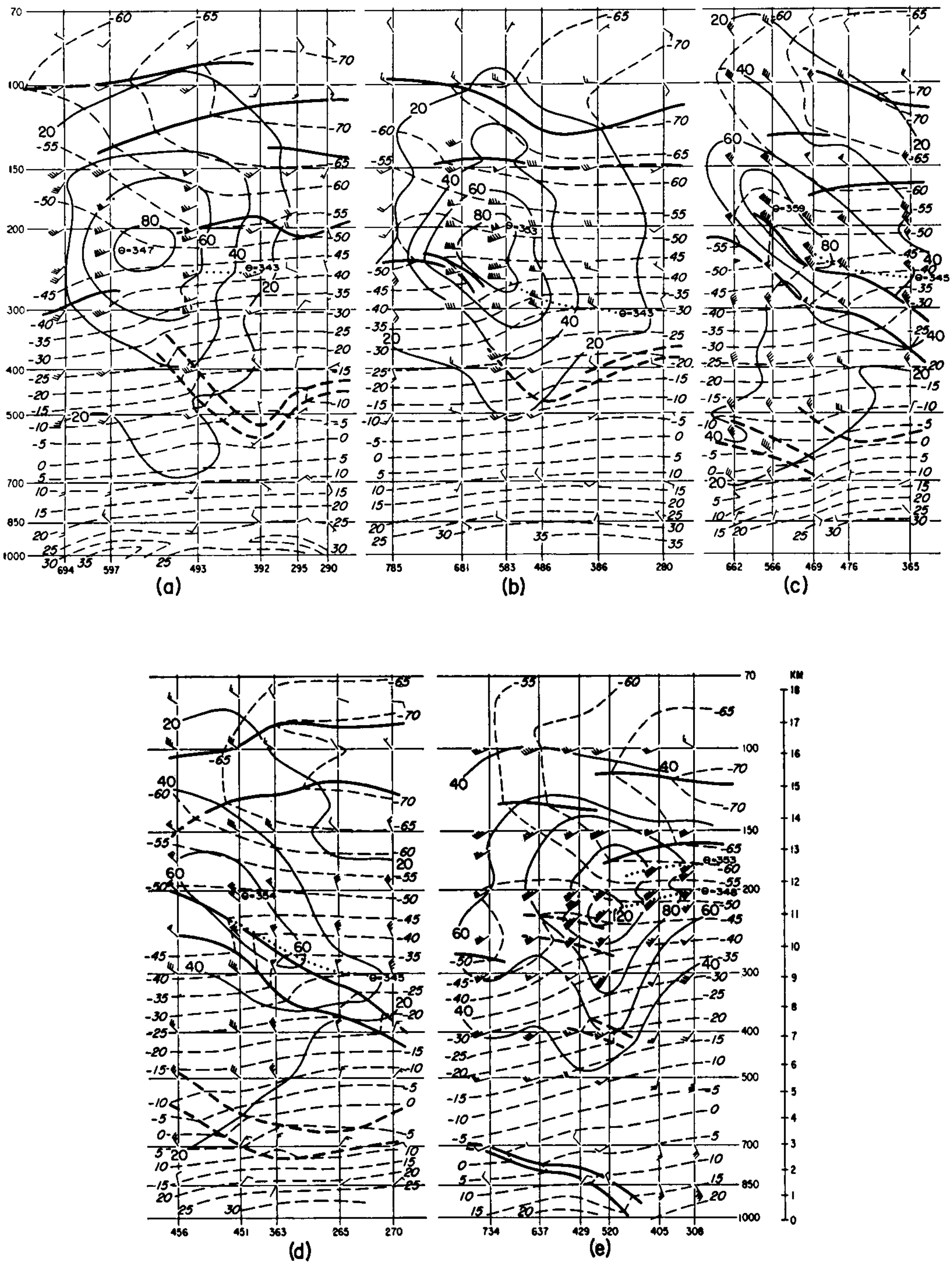

FIG. 10. Distributions of temperature and wind along lines indicated in Fig. 9.

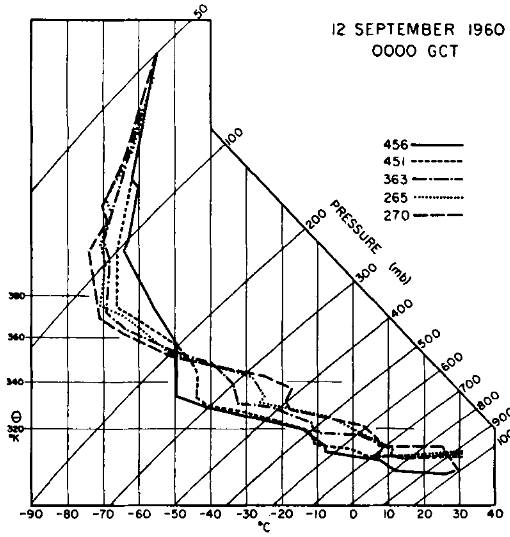

FIG. 11. Temperature soundings at stations in Fig. 10*d*.

level of maximum wind) and roughly 250 km north and south of that axis, were plotted against potential temperature (Fig. 12).

Where the winds were strong near the ridges (cf. Fig. 9), Fig. 12 suggests a reasonable conservatism of potential temperature near 345°K along the level of maximum wind. There appears to be a separate wind maximum higher up, the potential temperature of which seems also to be quasi-conservative along the direction of flow. Near the trough, where winds were weaker at lower levels, the upper wind maximum dominated and in some places obscured the presence of the lower-level jet.[1]

The apparent tendency for the level of maximum wind to follow isentropic surfaces over considerable distances (along a given streamline) is not surprising, in view of the strong reversal of shear otherwise required for an air particle to pass through the maximum-wind level.

The required conditions for this to take place may be appraised by use of the equation for the horizontal component of vorticity,

$$\frac{d\sigma}{dt} = -\sigma D_{xz} + \left(f - \frac{\partial u}{\partial y}\right)\frac{\partial v}{\partial z} - \frac{g}{T}\left(\frac{\partial T}{\partial x}\right)_p, \quad (7)$$

[1] At 150 mb, the isotach pattern differed considerably from that in Fig. 9, showing strongest winds a little west of the trough over the central United States.

Here x is taken along the direction of flow at the level concerned, the vorticity is expressed by the vertical shear $\sigma = \partial u/\partial z$, D_{xz} is the divergence in the x–z plane, and v is the wind component normal to the wind direction at the fiducial level. At the level of maximum wind, the first term on the right drops out.

Suppose that an element of air following an isentropic surface were to pass through the level of maximum wind from one layer where the shear is 10 m/sec per km to the other layer (above or below) where the shear is equivalent and of opposite sign. If such a change were accomplished in the relatively long time of 12 hr, $|\overline{d\sigma/dt}| \approx 5 \times 10^{-7}$ sec^{-2}.

To account for such a change, the last term in (7) would require an isobaric temperature gradient (along the direction of flow) of 15°C per 1000 km. At the jet core, the second term would require a value of $\partial v/\partial z$ (the component of vertical shear across the current) amounting to 5–6 m/sec per km, a much larger value being required on the anticyclonic flank but a smaller value on the cyclonic flank.

To see whether these requirements could be met, it is necessary to appeal to observations. Temperature gradients along the current, of the size mentioned above, do not appear to be present near the level of strongest wind. Weaker gradients are, of course, observed which would lead to some contribution from this term. With regard to the normal component of the wind, a synoptic-statistical study by Murray and Daniels (1951) revealed that although the cross-current shear is pronounced below and above jet level in entrance and exit regions of jet streams, it is weak or absent at jet level.

These observations are thus consistent with the tendency for the sheet of maximum wind to stream nearly along isentropic surfaces, following a given streamline. In the numerical example above, rather strong shears were assumed. Where the shears and the required changes of shear are smaller, the processes described by equation (7) may, however, cause air particles to traverse the level of maximum wind. It will be noted from Fig. 12 that it is only in regions of a strongly-peaked wind profile that the potential temperature is quasiconserved at the level of maximum wind.

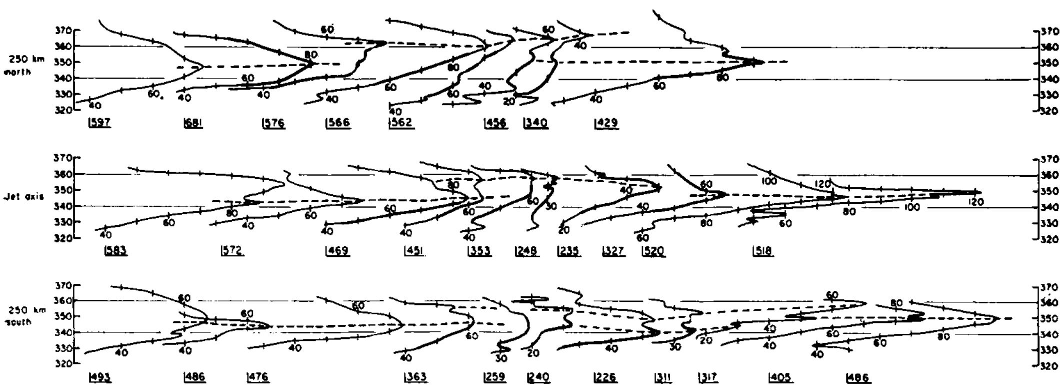

FIG. 12. Profiles of wind speed plotted against potential temperature, at stations near core of subtropical jet, and about 250 km north and south of it, at 00 GCT September 12, 1960. Wind speed (kt) indicated adjacent to individual profiles.

5. Subtropical jet and stratospheric wind maxima on January 31, 1961

Inertial wind layers in troposphere: At 00 GCT January 31, 1961 (Fig. 13), the crest of the subtropical jet stream was located fairly far north, over the central United States. This permits an analysis complete enough to illustrate a computation of the vertical shear in

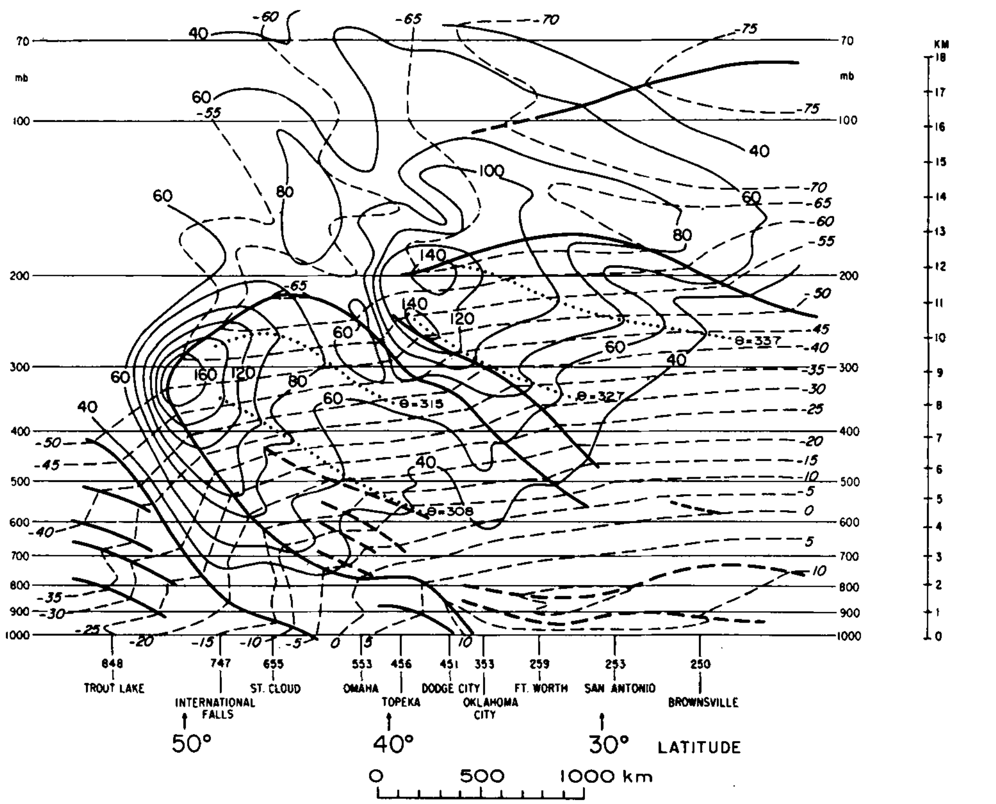

FIG. 13. Vertical section showing wind and temperature distribution near 95° W at 00 GCT January 31, 1961.

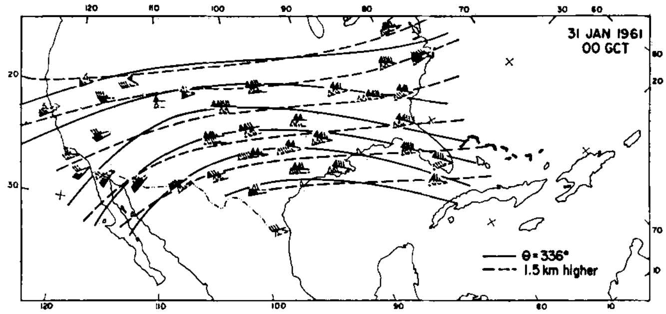

FIG. 14. Winds and streamlines (solid) at 336°K isentropic surface, and 1500 m above that surface (dashed), 00 GCT January 31, 1961.

relation to trajectory curvature. Attention will be focused upon the layer above the 337°K isentropic surface (Fig. 13) south of the subtropical jet, wherein the wind speed decreased with height despite a solenoidal field suggestive of an increase with height.

Within this layer, the following mean values are computed from the winds and temperatures at Fort Worth, San Antonio and Brownsville: $\partial V_g/\partial z = +2.2 \times 10^{-3}\,\mathrm{sec}^{-1}$, $\partial V/\partial z = -7 \times 10^{-3}\,\mathrm{sec}^{-1}$, $V = 38$ m/sec.

Curvatures were determined from streamlines at the 336°K isentropic surface (slightly below the level of maximum wind), and 1500 m above that surface. These indicate a marked decrease of anticyclonic curvature with height (Fig. 14). Over the whole region shown, the 336°K surface sloped downward toward south, indicating an increase of geostrophic wind with height. Inspection of Fig. 14 reveals that the observed wind speed generally decreased upward through this layer. The few exceptions (notably Midland, Brownsville and Burrwood) seen in the figure are accounted for by the fact that the upper surface in some places lay above the level of minimum wind and in the lower part of the layer of maximum wind higher up.

The geodesic curvature of the streamlines was determined by use of the formula given by Platzman (1947),

$$K_s = \partial\beta/\partial s + (\cos\beta \tan\varphi/a). \tag{8}$$

Here β is the wind direction measured counterclockwise from east, s is distance along the streamline, and a the earth's radius. The trajectory curvature was then computed from Blaton's formula,

$$K_T = K_s(V - c)/V,$$

where c is the celerity of the streamline system (8 m/sec in this case). The required values were taken from an analysis of the mean isogons for the layer shown in Fig. 14, which showed an anticyclonic curvature (with respect to the meridians) of 70° (or 1.23 radians) in a distance of 1600 km, The curvatures were computed to be:

$$K_s = -6.6 \times 10^{-7}\ \mathrm{m}^{-1}, \quad K_T = -5.3 \times 10^{-7}\ \mathrm{m}^{-1}.$$

The variation of streamline curvature with height is, according to (8),

$$\frac{\partial K_s}{\partial z} \approx \frac{\partial}{\partial z}\left(\frac{\partial\beta}{\partial s}\right) = \frac{\partial}{\partial s}\left(\frac{\partial\beta}{\partial z}\right).$$

With close approximation from Blaton's formula,

$$\frac{\partial K_T}{\partial z} = \frac{\partial K_s}{\partial z}\left(\frac{V-c}{V}\right).$$

Isopleths of the angular change of wind direction through the 1.5 km layer were drawn, and it was found that there was a variation of this quantity of 40° in a distance of 1700 km. This gives a value of $\partial K_T/\partial z = +2.2 \times 10^{-10}\mathrm{m}^{-2}$.

Insertion of the above values into equation (2) gave the following result, the values of the individual terms being provided so that the reader may see their relative sizes:

$$\frac{\partial V}{\partial z} = \frac{1}{(f + 2K_T V)}\left[f\frac{\partial V_g}{\partial z} - V^2\frac{\partial K_T}{\partial z}\right]$$

$$= \frac{1}{(0.73 - 0.40) \cdot 10^{-4}\,\mathrm{sec}^{-1}} \cdot$$

$$\cdot [(1.61 - 3.19) \cdot 10^{-7}\,\mathrm{sec}^{-2}]$$

$$= -5 \cdot 10^{-3}\,\mathrm{sec}^{-1}.$$

This compares fairly well with the observed shear, $-7 \times 10^{-3}\,\mathrm{sec}^{-1}$.

Below the level of maximum wind, there was little variation of curvature with height in this instance. The observed increase of wind speed with height in a 1.5 km deep layer below the 336°K surface between Fort Worth and Brownsville was about double the thermal shear. This is consistent with the fact that the quantity $(f + 2K_T V)$ in (2) was about half the size of f.

Directly above the jet axis, the horizontal temperature gradient was inadequate to support the strong decrease of wind speed observed. The average shear between Topeka and Oklahoma City in the 1.5 km deep layer above the 336°K surface was -10 m/sec per km, only a fifth of which could be accounted for by the thermal wind. A computation similar to that above provided somewhat of an overestimate of the decrease of wind with height.

No great accuracy is claimed for these computations, which are very sensitive to the exact values adopted for their ingredients. Nevertheless they clearly demonstrate that the variations of centripetal acceleration with height dominate the strophic balance and account for the very significant variance of the measured wind shear from the thermal wind.

There was evidence (see Fig. 13) of shallow layers of maximum wind sloping downward toward south, on the anticyclonic flank of the polar-front jet as well as of the subtropical jet stream. This was a common feature in the analyses performed in connection with this investigation. In most but not all cases, these ancillary sheets of maximum wind appeared to lie nearly along isentropic surfaces. Their superposition on a wind field dominated by the strong solenoid concentration of the polar-front zone makes these anomalies appear relatively weak. Nevertheless, departures from the thermal wind relationship are just as strong as in the subtropical jet. It seems likely that the remarkable examples of thin layers of strong wind near 700 mb, described by Gustafson (1953), are connected with extensive sloping

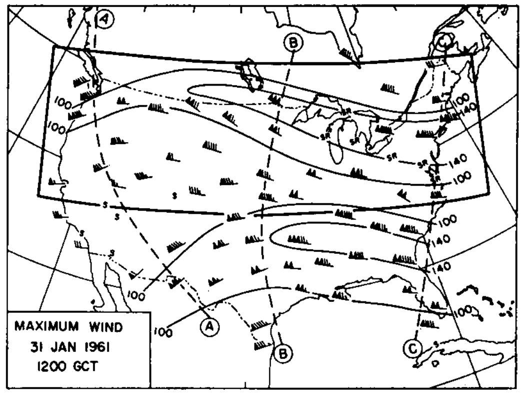

FIG. 15. Simplified isotachs (kt) at main level of maximum wind, 12 GCT January 31, 1961.

sheets of the kind seen in Fig. 13. Gustafson indicated the importance of inertial effects in accounting for the wind distributions he described.

Stratospheric wind maxima: In Fig. 13, wind maxima appear in the stratosphere above both the polar-front and subtropical jets. The general configuration of the isotachs at the primary "level" of maximum wind (near the tropopause) 12 hr later is shown by Fig. 15. Cross sections along lines A, B and C in this figure are shown in Fig. 16. These reveal remarkably well developed wind maxima, of restricted depth, in the stratosphere above the polar-front jet stream. The stratospheric thermal field, characterized by a general decrease of temperature toward north, indicates thermal wind shears either much weaker than or opposite in sign from the observed vertical shears.

Sawyer (1961), by use of frequent observations with a radarsonde theodolite, has convincingly demonstrated the presence of persistent maxima and minima in the vertical wind profile. In his theoretical treatment, he shows that these can only be explained on the basis of inertial oscillations "in which the primary balance is between the inertia, Coriolis effects and the static stability". Although the variations treated by Sawyer are of a much finer scale than these we describe here, there are no doubt similarities in their basic natures.

The wind profiles for three successive times are shown, for the quadrangle outlined in Fig. 15, in Fig. 17. As usual, some observations were terminated or interrupted in the region of strongest wind.

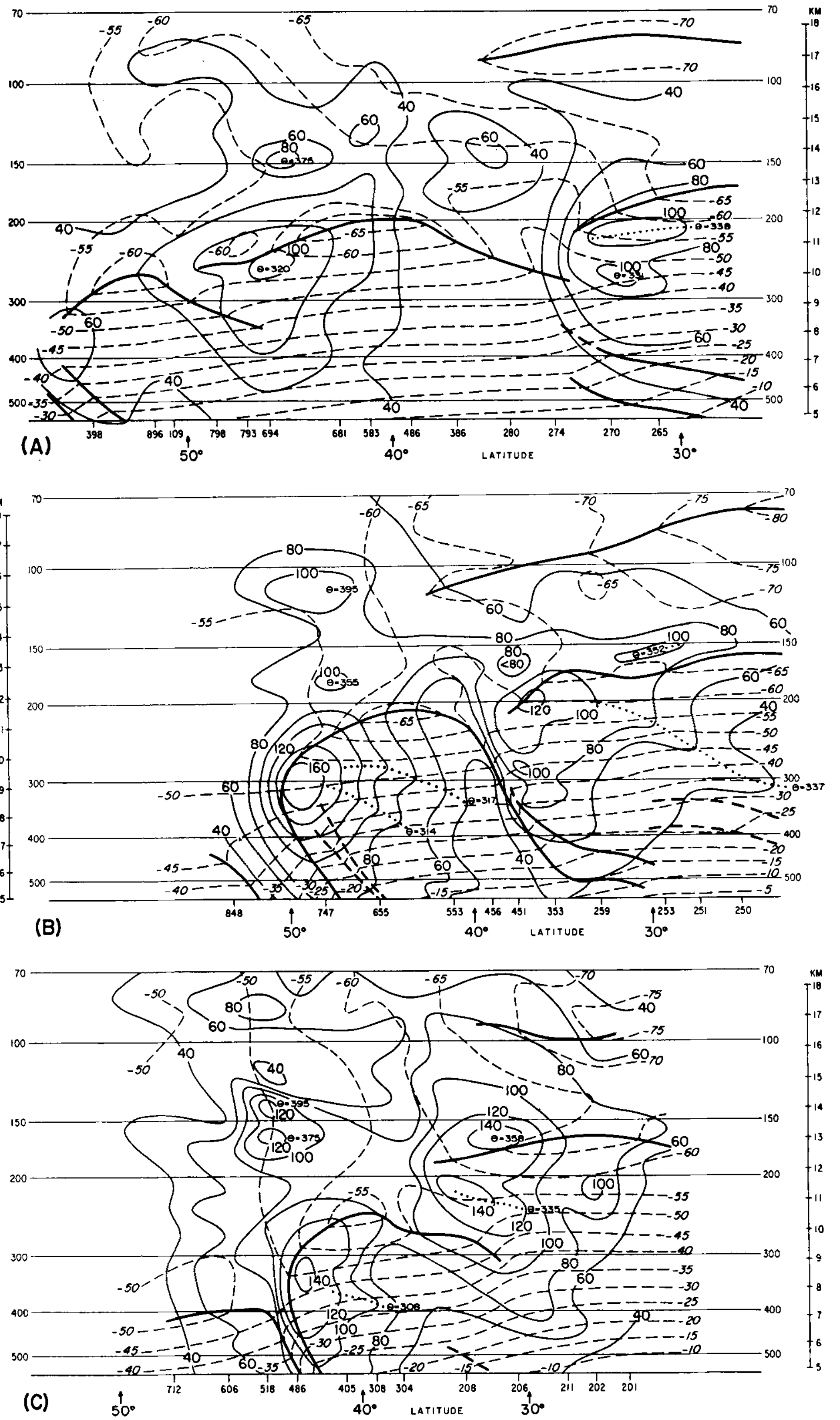

Fig. 16. Sections along lines A (top), B (middle) and C (bottom) in Fig. 15, showing distributions of wind speed and temperature.

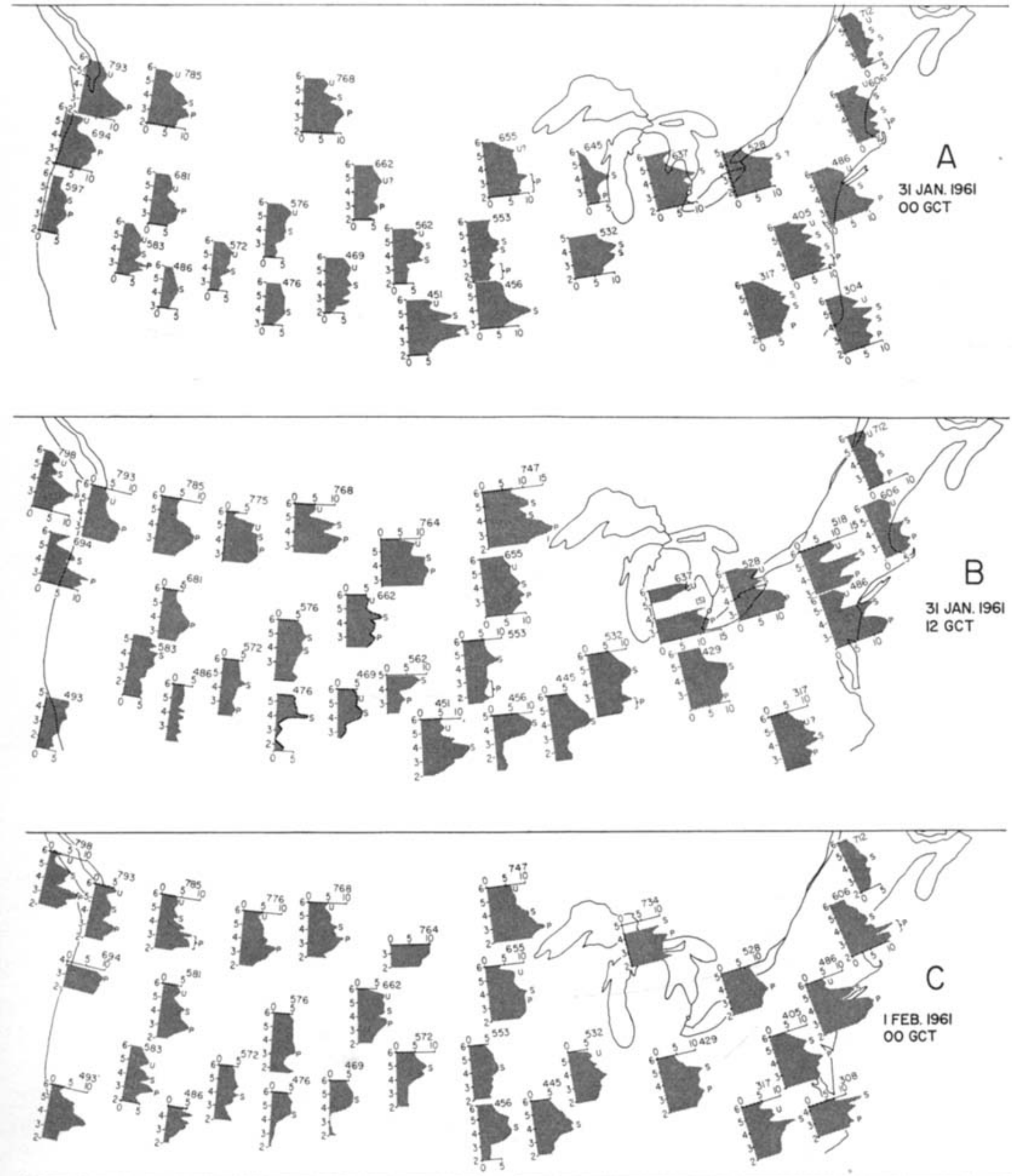

FIG. 17. Wind-speed profiles at (*a*) 00 GCT January 31, 1961; (*b*) 12 GCT January 31, 1961; and (*c*) 00 GCT February 1, 1961. Abscissas at individual stations, speed in tens of knots; ordinates, heights in tens of thousands of feet. See text.

Nevertheless, it is possible with the aid of cross sections and space and time continuity to identify certain features over a wide area. Maxima that could be identified with fair certainty are marked beside the individual wind profiles, as being either the polar-front jet (*P*), part of the northward extension of the subtropical jet (*S*), or an upper jet (*U*). In some cases, where a jet is undercut or overrun by another jet of considerable strength, appreciable shear appears only above or below the maximum concerned, or the weaker jet may be totally obscured.

A comparison of profiles (e.g., at stations 317, 528, 486, 518, 606, and 712 in Fig. 14*B*) reveals that individual features stand out with clarity in the region of strongest winds, but that their relative strengths vary considerably over the appreciable distances between observing stations. This is as would be expected from the scale of, say, the polar-front jet. Despite the chaotic appearance of the collection of profiles at first glance, it will be seen on careful scrutiny that each of the sheets of strongest wind can be recognized over a broad region.

Depending on the strength of his faith in the observations, one may or may not be confident in the reality of the wind-speed fluctuations shown in Fig. 17. At low elevation angles, small errors in angular measurements of balloon elevation can result in large apparent fluctuations of wind speed. Nevertheless, the fact that stratospheric wind maxima of the kind shown in Figs. 16 and 17 can be identified at several neighboring stations and at successive observation times, leads the writers to believe that they are essentially real.

6. Departures from thermal wind as related to inertial oscillations

Variations in wind speed along the jet stream, such as seen in Figs. 1 and 9, are a very stable feature of the subtropical jet stream. As Palmén (1954) has observed, the strongest winds are generally found in the crests of the subtropical jet, which in winter are located near the longitudes where the middle-latitude mean westerlies dip furthest south. Thus these maxima occur downstream from regions of large-scale confluence, as described by Namias and Clapp (1949). An analysis of three winter months by Krishnamurti (1960) revealed that the strongest winds in the subtropical jet tended to remain very steady from day to day, in locations corresponding closely to the longitudes of the three wind maxima appearing on Namias and Clapp's winter mean charts.

The contour, streamline and isotach pattern may be represented schematically as in Fig. 18, for a jet streak having maximum speed in the crest. In examining the characteristics of such jet streaks, it is convenient to consider variations in both the geostrophic and ageostrophic portions of the velocity. It is generally accepted that there is a correlation between actual wind speed and geostrophic wind speed, such that the isobaric contours are confluent in the "entrance" and diffluent in the "exit" regions upstream and downstream from the speed maxima. At the same time, as is well known, speed variations along the jet stream must be associated with flow having components alternately toward lower and higher contours. Thus in Fig. 18 the streamlines must have a greater amplitude than the contours. Consistent with equation (1), winds must be supergeostrophic in crests and subgeostrophic in troughs of the wave pattern.

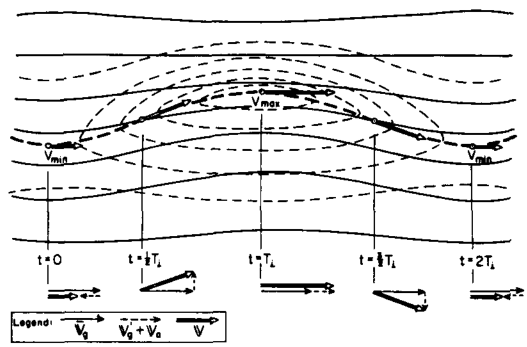

FIG. 18. Schematic contours (solid lines) and isotachs (dashed) corresponding to velocity field with maximum wind speed in crests of wave pattern. Arrows indicate wind velocities in various portions of the wave, for an air particle in the core of the jet stream. The wind oscillates about a mean velocity in the manner indicated in lower part of figure (see text). From Newton (1959).

The above considerations indicate that the geostrophic wind generally varies in the same sense as the actual wind, but that the latter varies at a greater rate. On this basis, Newton (1959) tested the hypothesis that, in the core of the jet stream, the vector wind velocity varies at twice the rate of variation of the geostrophic wind velocity.

With this simple assumption, an air particle in the core of the jet stream would undergo velocity fluctuations such as represented schematically by the arrows in Fig. 18. The variable part of the velocity, consisting partly of variations of geostrophic velocity and partly of the ageostrophic wind, is represented by a

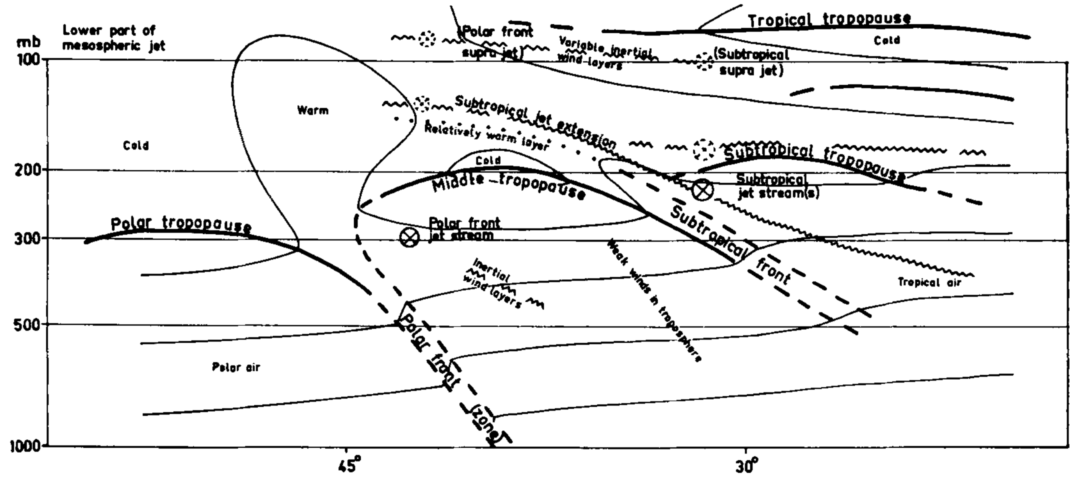

FIG. 19. Sketch of principal features of wind and temperature fields in middle and subtropical latitudes (most characteristic of crests of the subtropical jet stream). Isotherms are schematic, and do not necessarily represent any particular temperature interval.

vector which rotates anticyclonically in the same way as a purely inertial wind in a field of no (or constant) pressure gradient.

The period of such motion is a full pendulum day. The mean speed (minus the speed of progression of the jet streak) times the period of the oscillation must equal the wavelength. A test against Krishnamurti's data for the mean subtropical jet stream gave a good agreement, both in relating the speed to the wavelength and in accounting for the amplitude of meander of the jet stream about a mean latitude. Thus the conditions sketched in Fig. 18 appear to describe the inertial characteristics of the core of the jet stream. The amplitude of the meander of streamlines about a central contour is dependent on the size of the geostrophic departure, which is itself related to the speed variations along the current.

Such speed variations are presumably greatest near the level of maximum wind; consequently the geostrophic deviations decay above and below that level. The variation of ageostrophic wind with height is the main factor involved in producing strong vertical shear (equation 7). Thus the mechanism leading to the production of strong vertical shear inherently leads to a breakdown of the geostrophic thermal wind relationship.

Although no complete analysis can be made of the stratospheric wind maxima shown in Figs. 16 and 17, these are obviously tied up with strong inertial influences. In Fig. 16C, the wind speeds in the layers of strong and weak winds above the polar-front jet were of the order 20 to 40 kt larger or smaller than the geostrophic winds at the corresponding levels.

If the stratospheric jets are of the same general configuration as described by Fig. 18, it would be expected that in a particular layer the winds would be alternately super- and subgeostrophic, at different locations along the current. If the oscillations were purely inertial (variations in wind speed having no influence on the geostrophic wind field), the period of an oscillation would be at this latitude about 17 hr. With a mean wind speed of 80 kt at a given level a velocity streak would then have a length of the order 2500 km. Since the sections in Fig. 16 are about half that distance apart, this would be consistent with the presence of a wind maximum at a particular potential temperature on one section, and its failure to appear on all. Since the relation between real and geostrophic speed variations along the current is not known, the length of a jet streak may be longer or shorter than indicated above.

7. Summary

A sketch is given in Fig. 19, summarizing in schematic form the features of the wind and temperature fields most persistently identified in our analyses of winter cases. As noted earlier, the degree of development of individual features varies greatly from case to case, and in some instances a particular feature may appear to be absent or ill-defined. Those for which this is often true are marked as dashed lines in the figure.

The principal tropopauses which are always present in strength are the polar, middle and tropical tropopauses, in accord with the scheme of Mohri (1953; 1958) and of Defant and Taba (1957). The subtropical tropopause is generally quite distinct, but occasionally attenuated, especially on its equatorward side. One or more lower tropical tropopauses are generally present, below the one marking the coldest temperatures in the tropical air.

The subtropical front, having as its base the equatorward extension of the middle tropopause and sometimes extending as low as 500 mb, is occasionally as strong as the polar front. More often, its base is identifiable as a lapse-rate discontinuity but its top is more diffuse. North of the tropopause break, an inversion above the middle tropopause extends up to a sloping warm layer which may be identified all the way north to the warm band on the poleward side of the polar front.

The subtropical jet frequently appears as two layers of maximum wind. The lower of these lies within the tropopause break, and slopes downward toward south, often being closely identified with an isentropic sheet. The upper one often lies above the subtropical tropopause. Either of these may be the stronger on a particular occasion, however, the upper layer always appears to be strongest in lower latitudes (more than 1000–1500 km south of the jet axis).

On the north side, a layer of maximum wind lies immediately above the aforementioned warm layer in the stratosphere, often being identifiable as far north as the polar-front jet. Nearly above the polar-front jet, the wind may be stronger in this layer than it is further south, but a connection with the subtropical jet may generally be discerned.

Below the tropical tropopause, another maximum-wind layer is often present, and this appears in many cases to extend north of the polar-front jet. On occasion, within this layer distinct filaments of locally stronger winds may be seen, resulting in the presence of polar-front and subtropical "supra-jets".

The broad-scale structure of the wind field is qualitatively in accord with the thermal field. Within restricted layers, the actual vertical shear differs appreciably, and may be opposite in sign, from the thermal wind. In general, where winds are strong large deviations from the thermal shear are found. These are accounted for by inertial effects, which result in a much larger percentual deviation of the vertical shear from the geostrophic shear, than of the wind speed at a given level from the geostrophic speed.

The presence of the subtropical jet extension, and of the supra-jet in the stratosphere above the polar-front jet, may either take the form of distinct stratospheric jets, or of a failure of the wind speed to decrease as strongly above the polar-front jet core as it should according to the thermal wind relationship.

REFERENCES

Bellamy, J. C., 1941, The use of pressure altitude and altimeter corrections in meteorology. *J. Meteor.*, **2**, pp. 1–79.

Bjerknes, J., 1951, Extratropical cyclones. In *Compendium of Meteorology*, Boston, Amer. Meteor. Soc., pp. 577–598.

Bundgaard, R. C., and collaborators, 1956, The Black Sheep system of forecasting winds for long-range jet aircraft. U. S. Air Force, *Air Wea. Serv. Tech. Rep.* **105–189**, 48 pp.

Defant, F., and Taba, H., 1957, The threefold structure of the atmosphere and the characteristics of the tropopause. *Tellus*, **9**, pp. 259–274.

Forsythe, G. E., 1945, A generalization of the thermal wind equation for arbitrary horizontal flow. *Bull. Amer. Meteor. Soc.*, **26**, pp. 371–375.

Gustafson, A. F., 1953, On anomalous winds in the free atmosphere. *Bull. Amer. Meteor. Soc.*, **34**, pp. 196–201.

Krishnamurti, T. N., 1961, The subtropical jet stream of winter. *J. Meteor.*, **18**, pp. 172–191.

Mohri, K., 1953, On the fields of wind and temperature over Japan and adjacent waters during winter of 1950–1951. *Tellus*, **5**, pp. 340–358.

Mohri, K., 1958, Jet streams and upper fronts in the general circulation and their characteristics over the Far East (part I). *Geophys. Mag.* (Tokyo), **9**, pp. 45–126.

Murray, R., and Daniels, S., 1951, Transverse flow at entrance and exit to jet streams. *Quart. J. Roy. Meteor. Soc.*, **79**, pp. 236–241.

Namias, J., and Clapp, P. F., 1949, Confluence theory of the jet stream. *J. Meteor.*, **6**, pp. 330–336.

NEWTON, C. W., 1959, Axial velocity streaks in the jet stream: Ageostrophic "inertial" oscillations. *J. Meteor.*, **6**, pp. 638–645.

PALMÉN, E., 1948, On the distribution of temperature and wind in the upper westerlies. *J. Meteor.*, **5**, pp. 20–27.

PALMÉN, E., 1954, Über die atmosphärischen Strahlströme. Inst. f. Meteor. u. Geophys. d. Freien Univ. Berlin, *Met. Abh.*, **2**, pp. 35–50.

PLATZMAN, G. W., 1947, Some remarks on the measurement of curvature and vorticity. *J. Meteor.*, **4**, pp. 58–62.

REITER, E. R., 1960, The detailed structure of the atmosphere near jet streams. *Geofisica Pura e Applicata*, **46**, pp. 193–200.

RIEHL, H., 1948, Jet stream in the upper troposphere and cyclone formation. *Trans. Amer. Geophys. Un.*, **29**, pp. 175–186.

SAUCIER, W. J., BRUNDIDGE, K. C., CUNNINGHAM, N. W., DUGSTAD, I., GOLDMAN, J. L., SANFORD, T. E., and SASAKI, Y., 1958, *Wind field near the tropopause*, Final Report, Contr. AF 19(604)–1565, A. and M. Coll. of Texas, 140 pp.

SAWYER, J. S., 1961, Quasi-periodic wind variations with height in the lower stratosphere. *Quart. J Roy. Meteor, Soc.*, **87**, pp. 24–33.

VÄISÄNEN, A., 1954, Comparison between the geostrophic and gradient wind in the case of westerly jet. *Geophysica* (Helsinki), **4**, pp. 203–217.